The Formation of Pitted Features on the International Simple Glass during Dynamic Experiments at Alkaline pH

Adam J. Fisher[1], Neil C. Hyatt[1], Russell J. Hand[1] and Claire L. Corkhill[1]

[1]*NucleUS Immobilisation Science Laboratory, Department of Materials Science and Engineering, The University of Sheffield, S1 3JD, UK.*

ABSTRACT

The forward rate of dissolution of the International Simple Glass (ISG) was determined under alkaline conditions at 40 ^{o}C using the Single Pass Flow Through (SPFT) method. Forward rates were consistent with those obtained in the literature for this glass composition. The formation of altered gel layers and surface pits was observed on the surface of glass particles, especially at the very highest pH values, despite the application of high flow rates to prevent the build-up of solubility limiting phases. These features could be attributed to preferential localized dissolution at sites with a higher alkali concentration or from a separate, less durable, vitreous phase. These results may indicate that surface pit and altered gel formation occurs under the forward rate of dissolution as imposed by the SPFT method, particularly for simplified borosilicate glass materials.

INTRODUCTION

The International Simple Glass (ISG) was developed as a standard material for international researchers to use to advance glass corrosion understanding in a coordinated approach [1]. The ISG is a six-component, non-radioactive alumino-borosilicate reference glass, with a composition simplified from the French inactive surrogate of the R7T7 nuclear waste, SON68. The ISG has been studied extensively, with the objective to understand glass corrosion mechanisms at a fundamental level and to underpin predictions of the long-term durability of nuclear waste glass over geological timescales in an underground repository.

Here, the surface morphology of ISG particles were examined after being subjected to dissolution at pH(RT) 7, 9 and 11, at 40°C, using the Single Pass Flow Through method [2], which is commonly used to determine the forward rate of glass dissolution for input to glass dissolution models.

EXPERIMENTAL DETAILS

The ISG was fabricated in 2012 by the MoSci Corporation in several batches (Rolla, MO, USA) [3]. The lot number of the batch used in this investigation was L1201 2601-M1205 0803, which was shown to be x-ray amorphous and single phase [4]. The nominal composition is reported as: 56.2 SiO_2, 17.3 B_2O_3, 12.2 Na_2O, 6.1 Al_2O_3, 5 CaO & 3.3 ZrO_2 wt.% [5]. Crushed glass particles (75 – 150 μm diameter) were produced and washed according to the Single Pass Flow Through (SPFT) ASTM C1662-10 standard [2]. The SPFT method is a standard dynamic dissolution test where fresh solution constantly flows over a sample to maintain dilute conditions. Under such conditions, glass dissolution is sustained in the forward rate, negating solution feedback effects and preventing alteration layer formation. Experiments were performed at 40 ^{o}C and in buffered solutions [6] at pH(RT) 7, 9 and 11. The solution flow rate (q) to glass surface area (S) ratio (q/S, m s^{-1}) was selected to sustain glass dissolution of the ISG in the forward rate [6, 7]. Table 1 shows the range of conditions applied within the experiments, which were performed in duplicate.

Table 1. Parameters applied during Single Pass Flow Through experiments using the International Simple Glass, and the forward dissolution rates determined for boron and silicon.

Temp / °C	pH (RT)	pH (T)	Buffer solution	ISG mass (g)	Flow-rate / ml d^{-1}	Test duration / d	$\log_{10}[q/S$ /m s$^{-1}]$	Steady-state reached / d	Forward-rate / 10^{-2} g m^{-2} d^{-1}		
									B	Si	Na
40	7	6.57	TRIS	0.44	80	100	-7.00	10 (B) 25 (Si)	0.51 ± 0.14	0.01 ± 0.007	-
40	9	8.67	TRIS	1	10	43	-8.26	21	1.30 ± 0.26	1.10 ± 0.22	1.09 ± 0.29
40	11	10.89	LiOH & LiCl	0.29	80	100	-6.81	35	6.01 ± 0.50	12.5 ± 2.1	11.15 ± 0.89

Effluent samples were collected at regular intervals and flow-rates were determined gravimetrically. The elemental release was measured by analyzing effluent solution for Si, B and Na concentrations using Inductively Coupled Plasma-Optical Emission Spectroscopy (ICP-OES, ThermoScientific iCAPDuo6300). All experiments were performed until the normalised B, Si and Na dissolution rates attained steady-state conditions according to ASTM C1662-1 and where at least three dissolution rate measurements near the end of the test did not deviate by >15% from their mean value for steady state to be achieved [7]. Additionally, the criterion that the sample should not lose more than 30% of its original surface area was applied [7]. The mean dissolution rate from ≥3 measurements at steady-state for each test was then recorded. Dissolution rates were calculated according to:

$$r_0 = \frac{(c_i - c_{i,o})q}{f_i S} \quad (1)$$

where r_0, represents the normalised dissolution rate of element, i, (where i = Si, B or Na) in g m^{-2} d^{-1}, c_i the concentration of element, i, in the effluent solution (mg L^{-1}), $c_{i,o}$ is the background concentration of element, i, in the input buffer solution (mg L^{-1}), q is the solution flow-rate (m^3 d^{-1}), S the surface area of the glass sample (m^2) and f_i the mass fraction of element i in the glass (unitless). Since the surface area, S, changes throughout the duration of the experiment as the glass dissolves, a surface area correction model [8] was applied to calculate the change in S. This was applied to all experimental data. Uncertainty in the experimentally obtained dissolution rates was calculated as the standard deviation of the sum of uncorrelated random errors [6]. Post-dissolution particles were analyzed by scanning electron microscopy (SEM) using a Hitachi TM3030 SEM operating at an accelerating voltage of 15 kV. Backscattered electron images were collected.

RESULTS AND DISCUSSION

The attainment of steady-state dissolution and forward rates are presented in Figure 1 and Table 1, respectively. Steady-state conditions were met after 10 d for boron and 25 d for Si at pH(RT) 7 (Fig. 1a). An increase in forward dissolution rate with increasing pH values was observed, as expected, due to elevated silica solubility with increasing alkalinity. Obtained forward rates were comparable with those reported in the literature, also measured by SPFT [7, 9].

Inspection of ISG particles by SEM after the attainment of steady-state dissolution at 40 °C at pH(RT) 7 and 9 reveal the presence of dehydration cracking and oval shaped pits < 10 μm in diameter (Fig 2). These features were also present, but to a greater extent, on ISG particles from the experiments at pH(RT) 11, where pits <50 μm in diameter were observed, in addition to deep curved troughs (Fig. 3). It is postulated that the oval shaped pits observed in Fig. 2 are a precursor for the trough features observed in Fig. 3, consistent with greater reaction progress at pH 11 when compared with pH 7 and 9. The pits formed at pH(RT)11, shown in Fig. 3d, appear to be surface pits overlain by an altered gel layer, while the cracks observed at the same pH in Fig. 3a are similar in nature to dehydrated silica gels previously observed in glass dissolution experiments [10].
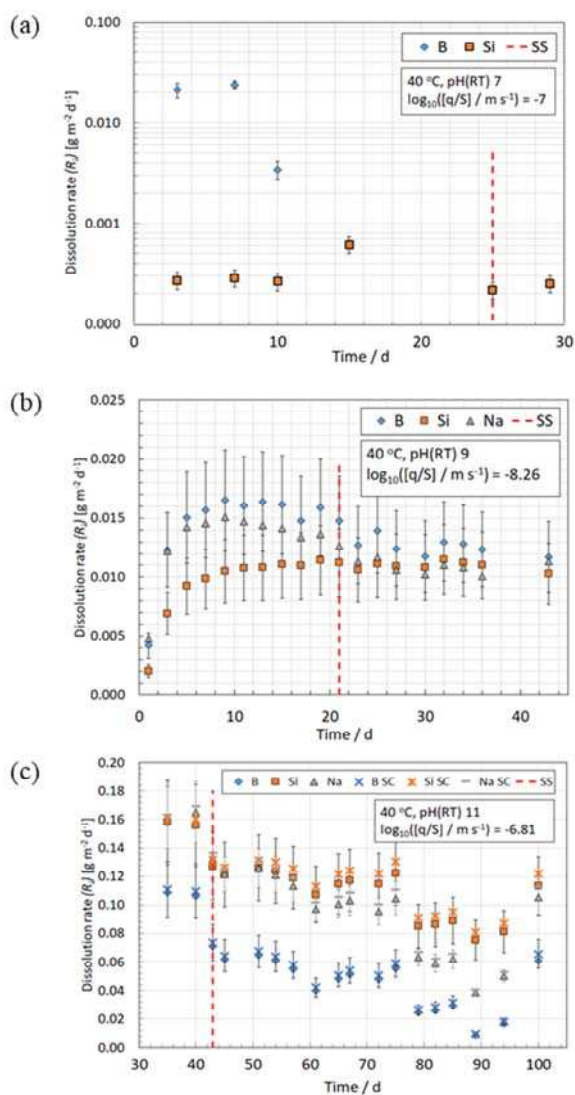
Figure 1. Dissolution rates in g m^{-2} d^{-1} as a function of time for (a) pH 7; (b) pH 9 and; (c) pH 11. The shrinking core model (SC) was applied in all cases, however, this only had a noticeable impact at pH 11. The steady state (SS) dissolution rate is marked at each pH by a red dashed line.

Cracked hydrated altered layers have previously been observed on the surface of glass particles under SPFT conditions; these were postulated to arise from preferential local attack [8, 10]. Gel layers were also observed at the highest pH values, indicating that chemical alteration occurs at the surface. The presence of gel layers could indicate that the q/S values employed in the SPFT experiments were not high enough to prevent the accumulation of silica in solution, especially at the highest pH values where its solubility is considerably elevated. It is thus possible that these experiments were not in true "forward rate" conditions, however,

gel layers were previously observed at the surface of glass particles in SPFT experiments in excessively dilute conditions, where flow rates were in excess of 200 ml d^{-1} [11], 2.5 - 20 times higher than those employed in the present study. The absence of a clear plateau in the q/S "sweep", which would indicate "forward rate" conditions for ISG [6, 7], makes it difficult to assess whether our experiments are in the "forward rate". If forward rate conditions were achieved in which elements are released from the glass congruently, the hypotheses of Geisler *et al.*[12], Hellmann *et al.* [13] and Putnis *et al.* [14] are supported, which propose that a silica-saturated boundary layer forms at the surface of the glass. Hence, the presence of an altered gel layer does not necessarily preclude the establishment of the forward dissolution rate conditions.   Pit and gel formation may be coupled: the pitted features may represent sites of lower chemical stability that preferentially dissolve, releasing elements to form a gel layer. The appearance of pitted features could be attributed to: (1) the dissolution of a separate crystalline or amorphous soluble phase [15]; or (2) a local pH increase in the solution trapped at the interface between the gel layer and the pristine glass [16-18]. The first possibility can be ruled out from this study as no separate soluble phase has been identified in ISG [4]. The second possibility could arise as a result of the presence of percolation channels in the medium range structural order of a glass (as defined by the modified random network model) as previously hypothesised by Jantzen [19]. If high alkali concentrated regions were to exist, when leached, they should increase the local leachate pH and form pits. These features could develop into troughs that follow the alkali channels.
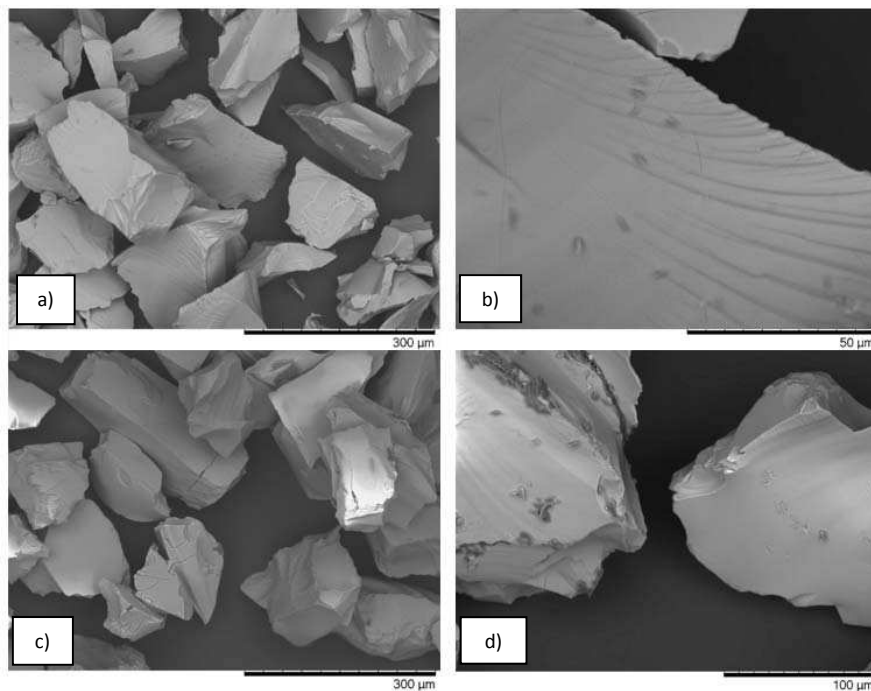

Figure 2. SEM images of (**a**) and (**b**) ISG particles after 100 days of dissolution at 40 °C and pH(RT) 7, at $\log_{10}(q/S$ m s^{-1}$)$ = -7; (**c**) and (**d**) ISG particulates after 43 days of dissolution at $\log_{10}(q/S$ / m s^{-1}$)$ = -8.26 at 40 °C and pH(RT) 9.
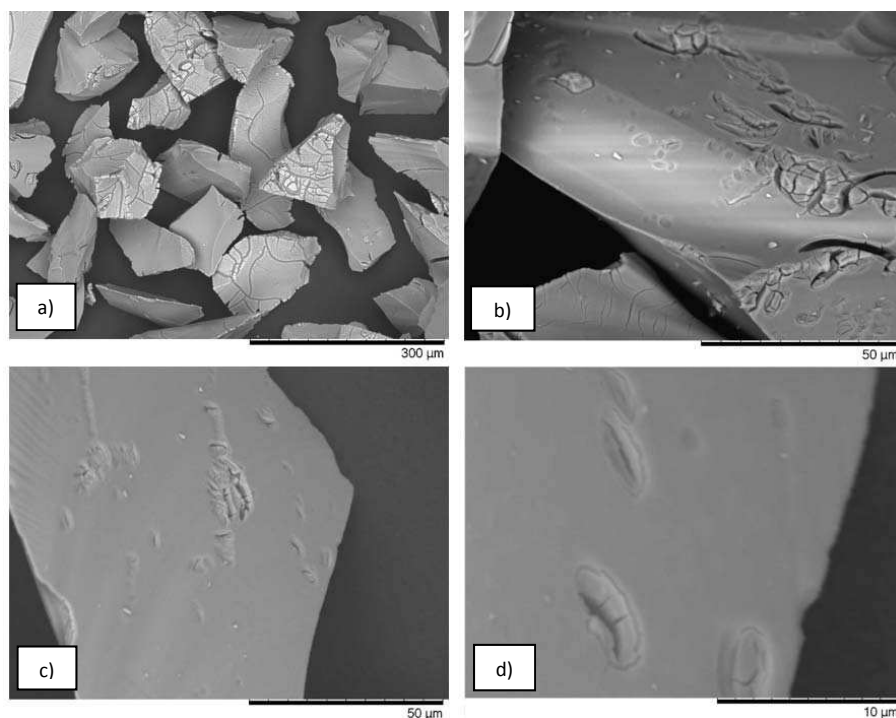
Figure 3. SEM images of ISG particles after 100 days of dissolution at 40 ºC and pH(RT) 11 at $\log_{10}(q/S$ m s$^{-1}) = -6.81$ showing **(a)** and **(b)** evidence for dehydration cracking and for localized preferential attack (pits and troughs); **(c)** trough formation possibly from the growth and coalescence of individual pits; and **(d)** high magnification image of pits covered by a dehydrated gel.

CONCLUSIONS

This investigation has revealed the presence of altered gel layers and pitted features on the surface of ISG particles after sustained dissolution in alkaline conditions, nominally at the forward-rate, by deployment of the SPFT methodology. This shows that gel layers may be formed in the forward rate of reaction, as imposed by this method, and that the formation of pitted features could be an intrinsic process in glass corrosion. This may be attributed to the structure of the glass network. Further work using grossly phase separated glass compositions could be performed to understand such behaviour further.

ACKNOWLEDGMENTS

REFERENCES

[1] S. Gin, A. Abdelouas, L. J. Criscenti, W. L. Ebert, K. Ferrand, T. Geisler, M. T. Harrison, Y. Inagaki, S. Mitsui, K. T. Mueller, J. C. Marra, C. G. Pantano, E. M. Pierce, J. V. Ryan, J. M. Schofield, C. I. Steefel and J. D. Vienna, *Mater. Today.* **16**, 243-248 (2013).

[2] ASTM Standard – 'Standard practice for measurement of the glass dissolution rate using the single-pass flow-through test method (SPFT)'; C1662-10, (2010).

[3] S. Gin, P. Jollivet, M. Fournier, C. Berthon, Z. Wang, A. Mitroshkov, Z. Zhu and J.V. Ryan, *Geo. Cos. Act.* **151**, 68-85 (2015).

[4] T. C. Kasper, C. Mann, M. Kirkham, J. D. Vienna, S. Gin, P. Frugier, M. T. Harrison, J. J. Neeway, J. V. Ryan   Invited review: Physical and optical properties of the International Simple Glass *Nat. Mat. Deg.* (2018) (in preparation).

[5] SRNL. Letter report on compositional measurements of common simple glass. Savannah River National Laboratory, SRNL-L3100-2012-00092 (2012).

[6] D. J. Backhouse, A. J. Fisher, C. L. Corkhill, N. C. Hyatt and R. J. Hand, *Nat. Mat. Deg.* **2**, 29 (2018).

[7] J. J. Neeway, P. C. Rieke, B. P. Parruzot, J. V. Ryan & R. M. Asmussen, *Geo. Cos.   Act.* **226,** 132-148 (2018).

[8] B. P. McGrail, W. L. Ebert, A. J. Bakel and D. K. Peeler, *J. Nuc. Mat.* **149**, 175-189 (1997).

[9] M. Fournier, A. Ull, E. Nicoleau, Y. Inagaki, M. Odorico, P. Frugier and S. Gin, *J. Nucl. Mater.* **476**, 140-154 (2016).

[10] E. Pierce, L. R. Reed, W. J. Shaw, B. P. McGrail, J. Icenhower, C. F. Windisch, E. A. Cordova and J. Broady, *Geo. Cos. Act.* **74**, 2634-2654 (2010).

[11] J. P. Icenhower. Private communication regarding the Nature Materials Degradation publication – D. J, Backhouse, A. J. Fisher, C. L. Corkhill, N. C. Hyatt and R. J. Hand, *Nat. Mat. Deg.* **2**, 29 (2018).

[12] T. Geisler, A. Janssen, D. Scheiter, T. Stephan, J. Berndt and A. Putnis, *J. Non-Cryst. Solids* **356**, 1458-1465 (2010).

[13] R. Hellman, R. Wirth, D. Daval, J. Barnes, J. Penisson, D. Tisserand, T. Epicier, B. Florin and R. L.   Hervig,   *Chem. Geol.* **294-295,** 203-216 (2012).

[14] A. Putnis and C.V. Putnis*, J. Solid. State. Chem.* **180**, 1783 (2007).

[15] J. P. Icenhower, B. P. McGrail, W. J. Shaw, E. M. Pierce, P. Nachimuthu, D. K. Shuh, E. A. Rodriguez and J. L. Steele, *Geo. Cos. Act.* **72**, 2767-2788 (2008).

[16] R. K. Chinnam, P. C. M. Fossati andW. E. Lee. *J. Nuc. Mat.* **503,** 56-65 (2018).

[17] Hench L.L & Clark D.E, "Surface properties and performance prediction of alternative waste forms," *Florida Univ., Gainesville* (1986).

[18] J. E. Mendel, "Final report of the defence high-level-waste leaching mechanisms program," *Pacific   Northwest National Laboratory* (1984).

[19] C. M. Jantzen, K. G. Brown and J. B. Pickett. *Int. J. App. Gla. Sci.* **1,** 38-62 (2010).